Fundamental limits on inferring epidemic resurgence in real time

Kris V. Parag[1,*] and Christl A. Donnelly[1,2]

[1]MRC Centre for Global Infectious Disease Analysis, Imperial College London, London, UK.

[2]Department of Statistics, University of Oxford, Oxford, UK.

*For correspondence: k.parag@imperial.ac.uk.

Abstract

We find that epidemic resurgence, defined as an upswing in the effective reproduction number (R) of the contagion from subcritical to supercritical values, is fundamentally difficult to detect in real time. Intrinsic latencies in pathogen transmission, coupled with often smaller incidence across periods of subcritical spread mean that resurgence cannot be reliably detected without significant delays, even if case reporting is perfect. This belies epidemic suppression (where R falls from supercritical to subcritical values), which can be ascertained 5–10 times more rapidly. These innate limits on detecting resurgence only worsen when spatial or demographic heterogeneities are incorporated. Consequently, we argue that resurgence is more effectively handled proactively, at the expense of false alarms. Responses to recrudescent infections or emerging variants of concern will more likely be timely if informed by improved syndromic surveillance systems than by optimised mathematical models of epidemic spread.

Keywords: reproduction numbers; infectious diseases; resurgence; real-time limits; models.

Introduction

Real-time estimates of the transmissibility of an infectious disease [1,2] are crucial for informed outbreak responses. Timely detection of salient changes in the effective reproduction number (R) of the disease of interest, which measures the average number of secondary cases likely caused by a primary case, can provide important evidence for policymaking and public communication [3,4], as well as improve forecasts of disease burden [5] (e.g., hospitalisations and deaths). Two critical changes of interest are *resurgence* and *control*. Resurgence, which we define as an increase from subcritical ($R \leq 1$) to supercritical ($R > 1$) transmissibility, can warn of imminent waves of infections, signify the emergence of pathogenic variants of concern and signal important shifts in the behavioural patterns of population [6,7]. Alternatively, control (or suppression) describes a switch from supercritical to subcritical spread and can indicate the effectiveness of interventions and the impact of depleting susceptibility (including that due to vaccine-induced immunity) [8,9].

Identifying these transmissibility changes in real time, however, is an enduring challenge for statistical modelling and surveillance planning. Inferring a transition in R from stochastic time

series of incident cases necessitates assumptions about differences among meaningful variation (*signal*) and random fluctuations (*noise*) [10–12]. Modern approaches to epidemic modelling and monitoring aim to maximise this signal-to-noise ratio either by enhancing noise filtering and bias correction methods [13–15], or by amplifying signal fidelity through improving surveillance quality and diversity [16–18]. While both approaches have substantially advanced the field, there have been few attempts to explore what, if any, *fundamental limits* exist on the timely detection of these changes. Such limits can provide key benchmarks for assessing the effectiveness of modelling or data collection and deepen our understanding of what can and cannot be achieved by real-time outbreak response programmes, ensuring that model outputs are not overinterpreted and redirecting surveillance resources more efficiently [19–21].

While studies are examining intrinsic bounds on epidemic monitoring and forecasting [22–25], works on transmissibility have mostly probed how extrinsic surveillance biases might cause R misestimation [14,26–28]. Here we address these gaps in the literature by characterising and exposing fundamental limits to detecting resurgence and control from a perfectly ascertained incidence time series. This provides vital insights into the best real-time performance possible and blueprints for how outbreak preparedness might be improved. We analyse a predominant real-time epidemic model [1,2] and discover stark asymmetries in our innate ability to detect resurgence and control. While epidemic control or suppression change-points are inferred robustly and rapidly, inherent delays (5–10 times that for control) strongly inhibit real-time resurgence estimation from widely used incidence curves or data.

We show that these fundamental constraints on resurgence worsen with smaller epidemic size, steepness of the upswing in R and spatial or demographic heterogeneities. Given this bottleneck to timely outbreak analysis, which exists despite perfect case reporting and the use of optimal Bayesian detection algorithms [15,29], we argue that methodological improvements to existing models used to analyse epidemic curves (e.g., cases, hospitalisations or deaths) are less important than enhancing syndromic surveillance systems [30,31]. Such systems, which fuse multiple data sources (including novel ones e.g., wastewater [32]) to triangulate possible resurgences might minimize some of these fundamental limitations. We conclude that early responses to suspected resurging epidemics, at the expense of false alarms, might be justified in many settings, both from our analysis and a consensus that lags in implementing interventions can translate into severely elevated epidemic burden [33–36]. Using both theory and simulation, we explore and elucidate these conclusions in the next section.

Results

Epidemic resurgence is statistically more difficult to infer than control

We first provide intuition for why resurgence and control might present asymmetric difficulties when inferring transmissibility in real time. Consider an epidemic modelled using a renewal branching process [37] over times (usually in days) $1 \leq s \leq t$. Such models have been widely applied to infer the transmissibility of numerous diseases including Ebola virus, COVID-19 and pandemic influenza. Renewal models postulate that the incidence of new cases at some time *s*, denoted I_s, depends on the effective reproduction number, R_s, and the past incidence, I_1^{s-1} as in **Eq. (1)** [2]. Here I_a^b means the set $\{I_a, I_{a+1}, \dots, I_b\}$ and $\equiv$ indicates equality in distribution.

$$\mathrm{P}(I_s | R_s, I_1^{s-1}) \equiv \mathrm{Pois}(R_s \Lambda_s), \qquad \Lambda_s = \sum_{u=1}^{s-1} w_u I_{s-u} \,. \quad (1)$$

In **Eq. (1)**, Pois represents Poisson noise and Λ_s is the total infectiousness, which summarises the weighted influence of past infections. The set of weights w_u for all *u* define the generation time distribution of the infectious disease with $\sum_{u=1}^{\infty} w_u = 1$ [38]. Applying Bayesian inference techniques (see [2,39] for derivations) under the assumption that transmissibility is constant over a past window of length *m* days, $\tau(s) = \{s, s-1, \dots, s-m+1\}$, we can obtain a gamma (Gam) distributed posterior distribution for R_s as $\mathrm{P}(R_s | I_1^s) \equiv \mathrm{Gam}\left(a + i_{\tau(s)}, \left(c + \lambda_{\tau(s)}\right)^{-1}\right)$, with (a, c) as prior distribution ($\mathrm{P}(R_s)$) parameters, $i_{\tau(s)} = \sum_{u \in \tau(s)} I_u$ and $\lambda_{\tau(s)} = \sum_{u \in \tau(s)} \Lambda_u$.

This posterior distribution only uses data up until time *s* and defines our real-time estimate of *R* at that time. We can analyse its properties (and related likelihood function $\mathrm{P}(I_1^s | R_s)$) to obtain the Fisher information (FI) on the left side of **Eq. (2)**. This FI (see [10,39] for derivation) captures how informative I_1^s is for inferring R_s, with its inverse defining the smallest asymptotic variance of any R_s estimate [10,40]. Larger FI implies better statistical precision.

$$\mathrm{FI}[R_s] = \frac{\lambda_{\tau(s)}}{R_s}, \qquad \mathrm{P}(R_s > 1 | I_1^s) = \sum_{j=0}^{a-1+i_{\tau(s)}} \frac{\left(c + \lambda_{\tau(s)}\right)^j}{j!} e^{-\left(c+\lambda_{\tau(s)}\right)}. \quad (2)$$

As resurgence will likely follow low incidence periods, we might expect $\lambda_{\tau(s)}$ to be small, while R_s rises. This effect will reduce the FI in **Eq. (2)**, making these changes harder to detect. In contrast, the impact of interventions will be easier to infer since these are often applied when cases are larger and reduce R_s. We expand on this intuition, using the *R* posterior distribution to derive the real-time resurgence probability $\mathrm{P}(R_s > 1 | I_1^s) = \int_1^{\infty} \mathrm{P}(R_s | I_1^s)\, dR_s$, as on the right side of **Eq. (2)**. We plot its implications in **Figure 1**, corroborating our intuition. In panel A we find that larger epidemic sizes improve our ability to detect shifts in transmissibility from

fluctuations in incidence (the posterior distributions for R_s overlap less). Panel B bolsters this idea, showing that when $\lambda_{\tau(s)}$ is smaller (as is likely before resurgence) we need to observe larger relative epidemic size changes ($\Delta\lambda_{\tau(s)} = \frac{i_{\tau(s)} - \lambda_{\tau(s)}}{\lambda_{\tau(s)}}$) for some increase in $\mathrm{P}(R_s > 1 |\, I_1^s)$ than for an equivalent decrease when aiming to detect control (where $\lambda_{\tau(s)}$ would be larger).

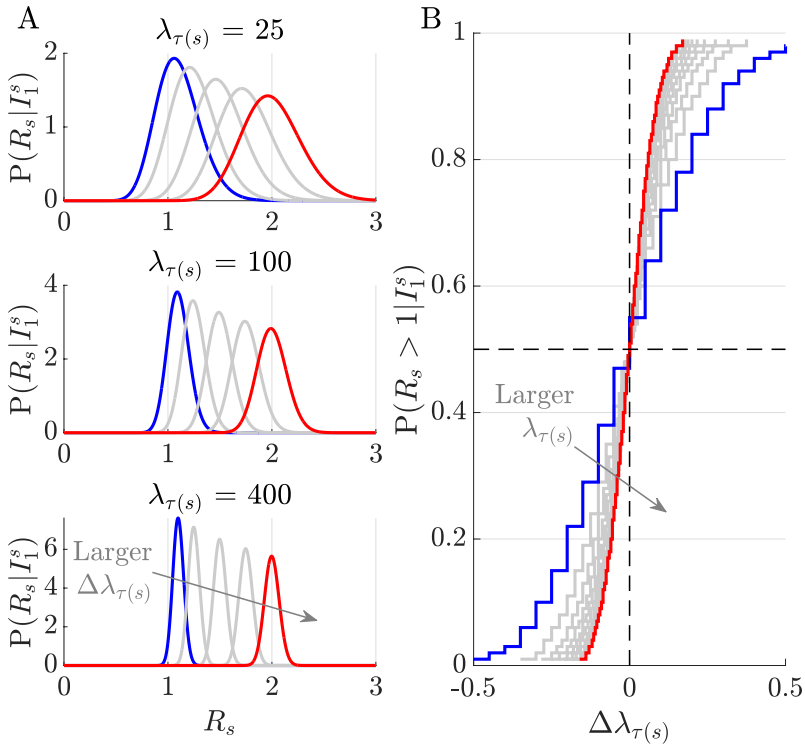

Figure 1: Relative sensitivity to perturbations in incidence. Panel A plots posterior real-time distributions for the effective reproduction numbers, R_s, at different relative incidence perturbations, $\Delta\lambda_{\tau(s)} = \frac{i_{\tau(s)} - \lambda_{\tau(s)}}{\lambda_{\tau(s)}}$, (increasing from blue to red). The degree of separation and hence our ability to uncover meaningful incidence fluctuations from noise, improves with the current epidemic size, $\lambda_{\tau(s)}$. Panel B shows how this sensitivity modulates our capacity to infer resurgence ($\mathrm{P}(R_s > 1 |\, I_1^s)$) and control ($\mathrm{P}(R_s \leq 1 |\, I_1^s) = 1 - \mathrm{P}(R_s > 1 |\, I_1^s)$). If epidemic size is smaller, larger relative incidence changes are needed to detect changes in R_s (curves have gentler gradient). Resurgence (likely closer to the blue line, top right quadrant) is appreciably and innately harder to detect than control (likely closer to the red line, bottom left quadrant).

Fundamental delays on detecting resurgence but not control

The intrinsic asymmetry in sensitivity to upward versus downward shifts in *R* (see **Figure 1**) implies that it is not equally simple to infer resurgence and control from incident cases. We investigate ramifications of this observation by comparing our real-time R_s-estimates to ones exploiting all the future incidence information available. We analyse two foundational posterior distributions, the *filtered*, p_s, and *smoothed*, q_s, distributions, defined in **Eq. (3)**. Here p_s considers information until time *s* and captures changes in R_s from I_1^s in real time. In contrast, q_s extracts all the information from the full incidence curve I_1^t, providing the best possible (in mean squared error) R_s-estimate [29]. The differential between p_s and q_s, summarised via the Kullback-Liebler divergence, $\mathrm{D}(p_s|q_s)$, measures the value of this future information.

$$p_s = \mathrm{P}(R_s|\, I_1^s), \qquad q_s = \mathrm{P}(R_s|\, I_1^t), \qquad \mathrm{D}(p_s|q_s) = \int_0^\infty p_s \log\frac{p_s}{q_s}\, dR_s. \quad (3)$$

Bayesian filtering and smoothing are central formalisms across engineering, where real-time inference and detection problems are common [29,41]. We compute formulae from **Eq. (3)** via the *EpiFilter* package [15,28], which employs optimal forward-backward algorithms. This method improves on the window-based ($\tau(s)$) formulation of the last section and maximises the signal-to-noise ratio in estimation. We also obtain filtered and smoothed probabilities of resurgence as $\mathrm{P}(R_s > 1 \mid I_1^s) = \int_1^\infty p_s\, dR_s$ and $\mathrm{P}(R_s > 1 \mid I_1^t) = \int_1^\infty q_s\, dR_s$. The probability that the epidemic is controlled (i.e., $R \leq 1$) is the complement of these expressions. Our main results, which average the above quantities over many simulated Ebola virus and COVID-19 epidemics, are given in **Figure 2** and **Figure 5** (appendix), respectively. We uncover striking differences in the intrinsic ability to infer resurgence versus control in real time.

Upward change-points are significantly harder to detect both in terms of accuracy and timing. Discrepancies between p_s- and q_s-based estimates (the latter benchmark the best realisable performance) are appreciably larger for resurgence than control. While decreases in *R* can be pinpointed reliably, increases seem fundamentally more difficult to detect. These limits appear to exacerbate with the steepness of the *R* upswing. We confirm these trends with a detailed simulation study across five infectious diseases in **Figure 3**. There we alter the steepness, θ, of transmissibility changes and map delays in detecting resurgence and control as a function of the difference in the first time that p_s- and q_s-based probabilities cross 0.5 (Δt_{50}) and 0.95 (Δt_{95}), normalised by the mean generation time of the disease. We find that lags in detecting resurgence are at least 5–10 times longer than for detecting control.

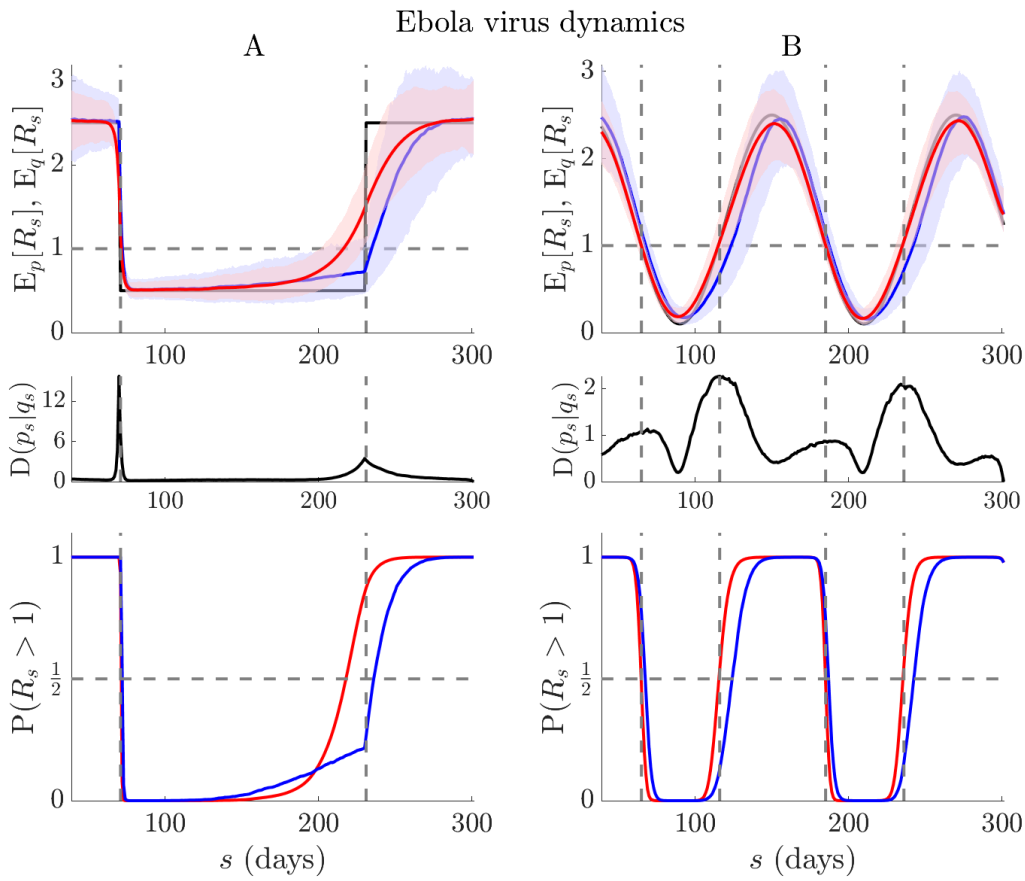

Figure 2: Resurgence and control dynamics of Ebola virus. Using renewal models with the generation time from [42], we simulate 1000 realisations of Ebola virus epidemics ($t = 300$) with step (A panels) and seasonally (B panels) changing transmissibility. Top panels plot mean estimates from the filtered ($\mathrm{E}_p[R_s]$, blue) and smoothed ($\mathrm{E}_q[R_s]$, red) distributions from every realisation (computed using *EpiFilter* [15]). Middle panels average the Kullback-Liebler divergences from those simulations and bottom panels present overall filtered ($\mathrm{P}(R_s > 1 \mid I_1^s)$, blue), and smoothed ($\mathrm{P}(R_s > 1 \mid I_1^t)$, red) resurgence probabilities. We find fundamental and striking delays in detecting resurgence, often an order of magnitude longer than those for detecting control or suppression in transmission (see lags between red and blue curves).

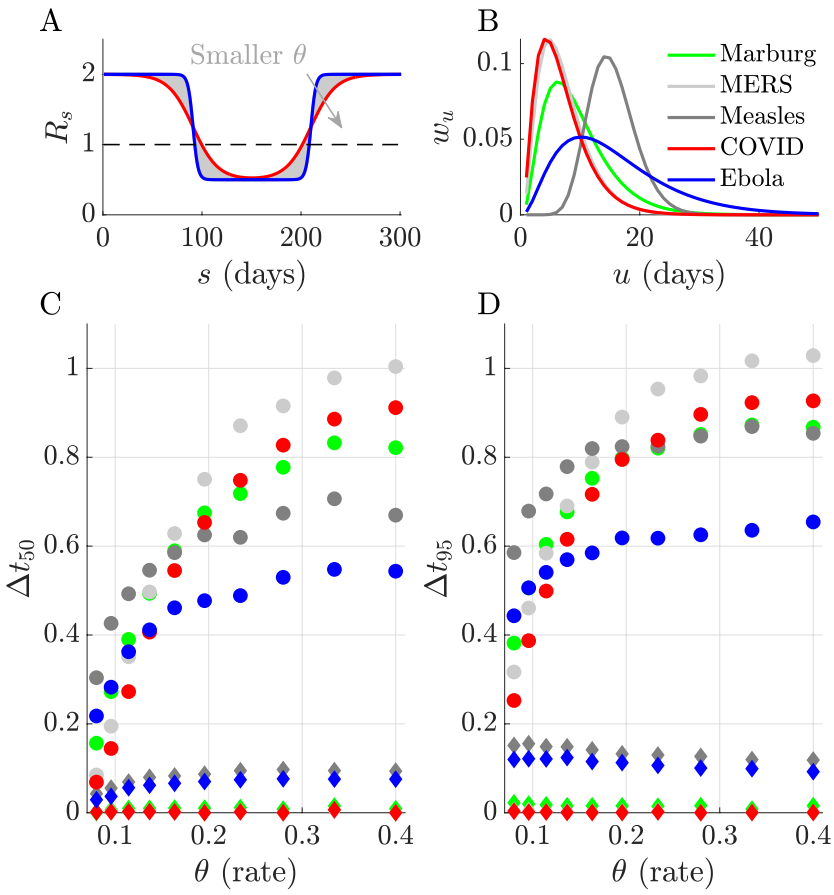

Figure 3: Delays in detecting upward and downward changes in *R*. We characterise the discrepancies between detecting resurgence and control against the steepness or rate, θ, of changes in transmissibility (R_s), which we model with logistic functions (panel A). We compare differences in the probability of detecting resurgence ($\mathrm{P}(R_s > 1)$) or control ($\mathrm{P}(R_s \leq 1)$ under filtered and smoothed estimates (see main text) first crossing thresholds of 0.5 (Δt_{50}) and 0.95 (Δt_{95}) for five infectious diseases (panel B plots their assumed generation time distributions from [2,42,43]). We simulate 1000 epidemics from each disease using renewal models and estimate R_s with *EpiFilter* [15]. Panels C and D (colours match panel B, Δt is normalised by the mean generation times of the diseases) show that delays in detecting resurgence (dots) are at least 5–10 times longer than for indicating control (diamonds). Our ability to infer even symmetrical transmissibility changes is fundamentally asymmetric.

Fundamental delays worsen with spatial or demographic heterogeneities

In previous sections we demonstrated that sensitivity to changes in *R* is asymmetric, and that intrinsic, restrictive limits exist on detecting resurgence in real time, which do not equally inhibit

detecting control. While those conclusions apply generally (e.g., across diseases), they do not consider the influence of spatial or demographic heterogeneity. We examine this complexity through a simple but realistic generalisation of the renewal model. Often *R*-estimates can be computed at small scales (e.g., at the municipality level) via local incidence or more coarsely (e.g., countrywide), using aggregated case counts [3,13]. We can relate these differing scales with the weighted mean in **Eq. (4)**, where the overall (coarse) *R* at time *s*, $\bar{R}_s$, is a convex sum of finer-scale *R* contributions from each group ($R_s[j]$ for the jth of *p* groups) weighted by the epidemic size of that group (as in **Eq. (2)** we use windows $\tau(s)$ for analytic insight).

$$\bar{R}_s = \sum_{j=1}^{p} R_s[j]\alpha_j\,, \qquad \alpha_j = \frac{\lambda_{\tau(s)}[j]}{\sum_{k=1}^{p}\lambda_{\tau(s)}[k]}\,. \quad (4)$$

Our choice of groupings is arbitrary and can equally model demographic heterogeneities (e.g., age-specific transmission), where we want to understand how dynamics within the subgroups influence overall spread [7]. Our aim is to ascertain how grouping, which often occurs naturally due to data constraints or a need to succinctly describe the infectious dynamics over a country to aid policymaking or public communication [44], affects resurgence detection. **Eq. (4)** implies that $\bar{R}_s - 1 = \sum_{j=1}^{p}(R_s[j]-1)\alpha_j$. Since resurgence will likely first occur within some specific (maybe high risk) group and then propagate to other groups [7], this expression suggests that an initial signal (e.g., if some $R_s[j] > 1$) could be masked by non-resurging groups (which are from this perspective contributing background noise).

As the epidemic size in a resurging group will likely be smaller than those of groups with past epidemics that are now being stabilised or controlled, this exacerbates the sensitivity bounds explored earlier via **Eq. (2)**. We can verify this further loss of sensitivity by examining how the overall posterior distribution depends on those of the component groups as follows, with $\circledast$ as a repeated convolution operation and Ω_j as the posterior distribution for the jth group.

$$R_s[j] \sim \Omega_j\big(i_{\tau(s)}[j], \lambda_{\tau(s)}[j]\big), \qquad \bar{R}_s \sim \circledast_{j=1}^{p}\,\alpha_j\Omega_j. \quad (5)$$

While **Eq. (5)** holds generally, we assume gamma posterior distributions, leading to statistics analogous to **Eq. (2)**. We plot these sensitivity results at $p = 2$ and 3 in **Figure 4** , where group 1 features resurgence and other groups either contain stable or falling incidence. We find that as *p* grows (and additional distributions convolve to generate $\bar{R}_s$) we lose sensitivity (posterior distributions overlap more for a given relative change in incidence ($\Delta\lambda_{\tau(s)}[1] = \frac{i_{\tau(s)}[1] - \lambda_{\tau(s)}[1]}{\lambda_{\tau(s)}[1]}$). Reductions in either the weight (α_1), epidemic size ($\lambda_{\tau(s)}[1]$) or other $R_s[j \neq 1]$, further

desensitise the resurgence signals i.e., decrease the gradient of detection probability curves. This is summarised by noting that if $R_s[1] = \max_j R_s[j]$, then the sensitivity from **Eq. (2)** is only matched when the resurging group dominates ($\alpha_1 \approx 1$) or if other groups have analogous R i.e., $R_s[1] \approx R_s[j]$. Delays in detecting resurgence can therefore be severe. Heterogeneity on its own, however, does not force asymmetry between detecting control and resurgence.

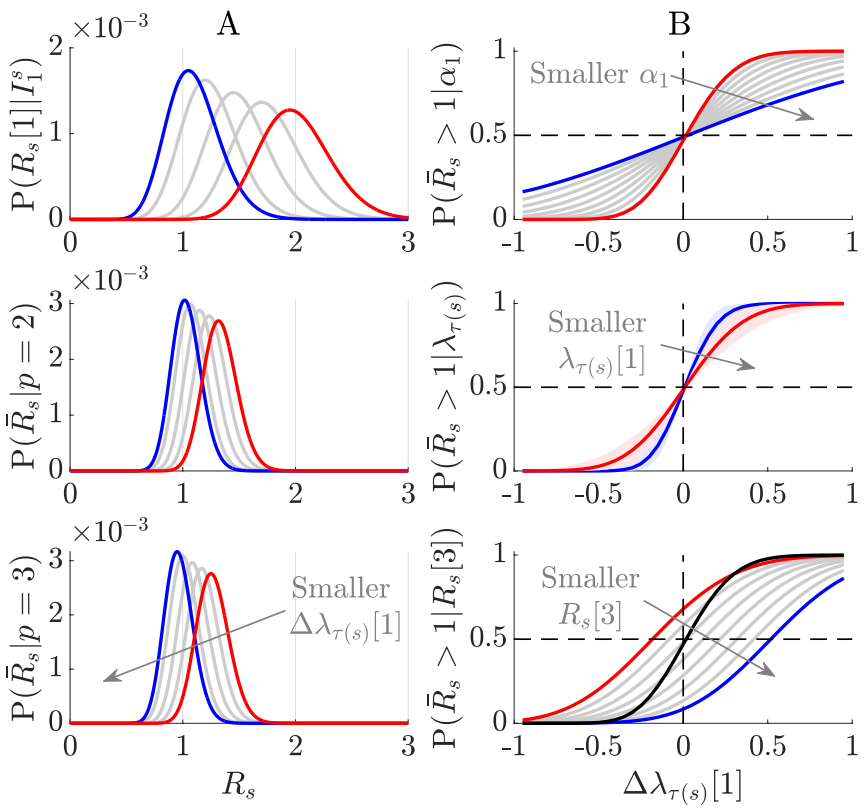

Figure 4: Influence of heterogeneities in transmission. We investigate how differences in transmissibility among groups (e.g., due to demographic or spatial factors) fundamentally limit the ability to detect resurgence from a specific group (in this example group 1). Panel A shows that the grouped posterior distribution becomes less sensitive to relative changes in group 1 incidence, $\Delta\lambda_{\tau(s)}[1] = \frac{i_{\tau(s)}[1] - \lambda_{\tau(s)}[1]}{\lambda_{\tau(s)}[1]}$ (increasing from blue to red). Posterior distributions over $\bar{R}_s$ are more overlapped (and tighter in variance) as p increases, for fixed $R_s[1]$ (top). Panel B plots how overall resurgence detection probability $\mathrm{P}(\bar{R}_s > 1)$ depends on the weight (α_1, top, 0.05–1) and epidemic size ($\lambda_{\tau(s)}[1]$, middle, 20–80, $p = 2$) as well as changes in $R_s[3]$ (bottom, 0.5–1.2, $p = 3$). Decreases in α_1 (red to blue) or $\lambda_{\tau(s)}[1]$ mean other groups mask the resurging dynamics in group 1, reducing sensitivity (curves become less steep). In the latter case the $\mathrm{P}(\bar{R}_s > 1)$ (red with solid line at median of $\lambda_{\tau(s)}[1]$ range) is always more

conservative than $\mathrm{P}(R_s[1] > 1)$ (blue, solid median line). As $R_s[3]$ falls (red to blue) the ability to detect resurgence also lags relative to that from observing group 1 (black).

Discussion

Probing the performance limits of noisy biological systems has yielded important insights into the real-time estimation and control of parameters in biochemistry and neuroscience [45–47]. Although models from these fields share dynamic similarities with those in epidemiology, there has been relatively little investigation of how real-time estimates of pathogen transmissibility, parametrised by *R*, might be fundamentally limited. This is surprising since *R* is among key parameters considered in initiatives aiming to better systematise real-time epidemic response [48,49]. Here we explored what limits may exist on our ability to reliably detect or measure the change-points in *R* that signify resurgence and control. By using a combination of Bayesian sensitivity analyses and minimum mean squared error filtering and smoothing algorithms, we discovered striking asymmetries in innate detection sensitivities.

We found that, arguably, the most crucial transitions in epidemic transmissibility are the most inherently difficult to detect. Specifically, resurgence, signified by an increase in *R* from below to above 1, can at earliest be detected 5–10 times later than an equivalent decrease in *R* that indicated control (**Figure 2**, **Figure *3*** and **Figure *5***). As this lag could be of the order of the mean generation time of the disease under study, even when case reporting is perfect and optimised detection algorithms are applied, this represents a potentially sharp bottleneck to real-time responses for highly contagious diseases. Intuition for this result came from observing that sensitivity to *R* change-points will weaken (due to noise masking the signal) with declining epidemic sizes and increasing 'true' *R*, both of which likely occur in resurgent settings (**Eq. (2)** and **Figure 1**). Furthermore, these latencies and sensitivity issues would only exacerbate when considering heterogeneous groupings across geography or demography (**Eq. (4), (5)** and **Figure 4**).

Practical real-time analyses would almost surely involve such groupings or data aggregations [9,13], in addition to being hindered by reporting and other latencies (e.g., if notification times, hospitalisations or deaths are used as proxies for incidence) [14,50]. Consequently, we argue that while case data provide robust signals for pinpointing when an epidemic is under control (and possibly disentangling the impact of interventions), they are insufficient, on their own, to sharply resolve resurgence timepoints. This does not invalidate the importance of approaches that do seek to better characterise real-time *R* changes [1,2,13,28], but instead adds context

on how such inferences should be interpreted when informing policy. Given intrinsic delays in inferring resurgence, which can associate with critical epidemiological changes, such as the emergence of variants of concern or important shifts in population behaviours [6,7], there are grounds for conservative approaches that enact interventions swiftly at the expense of false alarms. This might support, for example the ongoing COVID-19 policies of New Zealand and Australia [51], and adds impetus to recent studies showing how lags in the implementing of interventions can induce drastic costs [33–36].

Moreover, our analysis suggests that enhancing syndromic surveillance systems, which can comprehensively engage diverse data sources [30,31] may be more important than improving models for processing case data. Fusing multiple and sometimes novel data sources, such as wastewater or cross-sectional viral loads [18,32], may present the only truly realistic means of minimizing the innate limits to resurgence detection that we have demonstrated. Approaches aimed at enhancing case-based inference generally correct reporting biases or propose more robust measures of transmissibility, such as time-varying growth rates [14,49,52]. However, as our study highlights limits that persist at the gold standard of perfect case reporting and, further it is known that under such conditions growth rates and R are equally informative [53], these lines of investigation are unlikely to minimise the delays we have exposed.

There are two main limitations of our results. First, as we considered renewal model epidemic descriptions, which predominate real-time R studies, our work necessarily neglects the often-complex contact networks that mediate infection spread [54]. However, other analyses using somewhat different approaches to ours (e.g., Hawkes processes [55]) show apparently similar sensitivity asymmetries and there is evidence that renewal models can be as accurate as network models for inferring R [56], while being easier to run and fit in real time. Second, we did not include any explicit economic modelling. While this is outside the scope of this work it is important to recognise that resurgence detection threshold choices (i.e., how we decide which fluctuations in incidence are actionable) imply some judgment about the relative cost of true positives (timely resurgence detections) versus false alarms [12]. Incorporating explicit cost structures could mean that delays in detecting resurgence are acceptable. We consider this the next investigative step in our aim to probe the limits of real-time performance.

Appendix

We provide simulations in **Figure 5** for COVID-19, showing that significant delays in detecting resurgence but not epidemic control persist. These support **Figure 2** of the main text, which examined Ebola virus. While figures plot ensembles of mean estimates, single simulations

(where estimated credible intervals reflect noise from the incidence of that simulation) also display this asymmetry, confirming that real-time resurgence detection is innately hard.

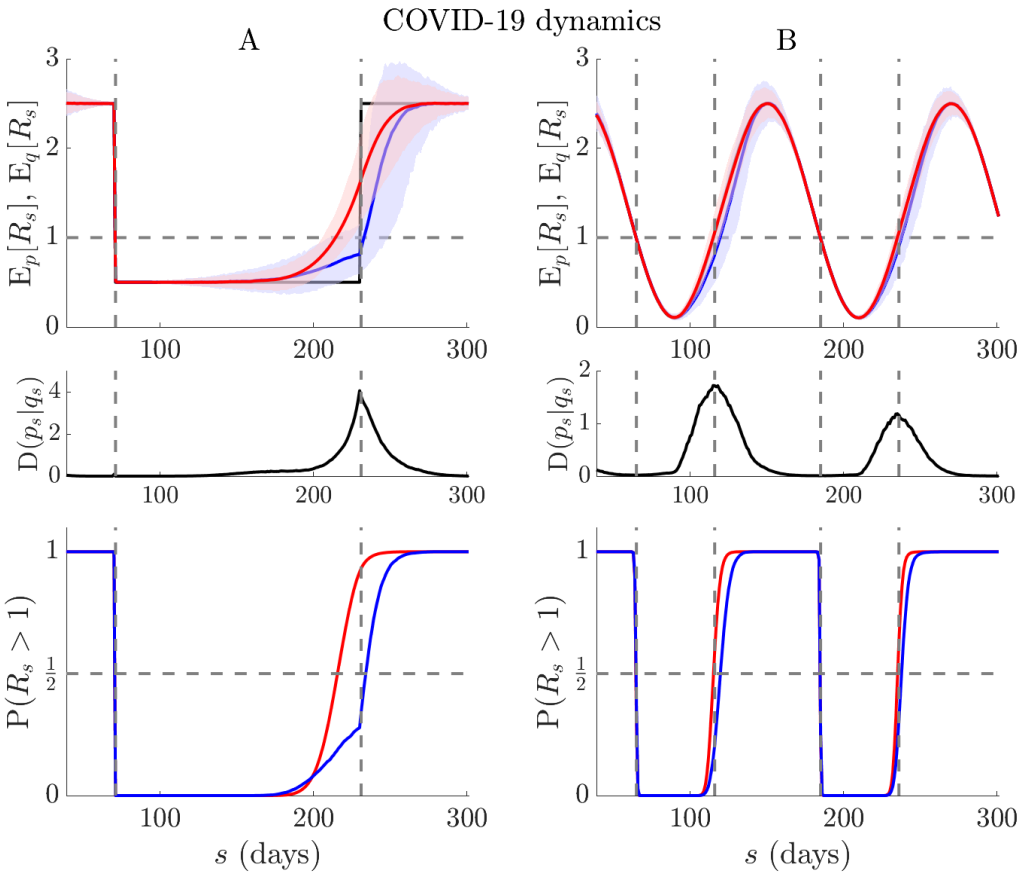

Figure 5: Resurgence and control dynamics of COVID-19. We repeat the simulations from **Figure 2** but for 1000 realisations of COVID-19 epidemics ($t = 300$) using generation times from [43]. Top panels plot posterior mean estimates from filtered ($\mathrm{E}_p[R_s]$, blue) and smoothed ($\mathrm{E}_q[R_s]$, red) distributions from every realisation (computed via *EpiFilter* [15]). Middle panels average Kullback-Liebler divergences from those simulations and bottom panels show overall filtered ($\mathrm{P}(R_s > 1 \mid I_1^s)$, blue), and smoothed ($\mathrm{P}(R_s > 1 \mid I_1^t)$, red) resurgence probabilities. We again find fundamental and appreciable latencies in detecting resurgence, often an order of magnitude longer than those for detecting epidemic control (compare red and blue curves).

Bibliography

1. Cauchemez S, Boëlle P-Y, Thomas G, Valleron A-J. Estimating in real time the efficacy of measures to control emerging communicable diseases. Am J Epidemiol. 2006;164: 591–597. doi:10.1093/aje/kwj274
2. Cori A, Ferguson NM, Fraser C, Cauchemez S. A new framework and software to estimate time-varying reproduction numbers during epidemics. Am J Epidemiol.

2013;178: 1505–1512. doi:10.1093/aje/kwt133
3. The R value and growth rate - GOV.UK [Internet]. [cited 1 Jul 2021]. Available: https://www.gov.uk/guidance/the-r-value-and-growth-rate
4. Li Y, Campbell H, Kulkarni D, Harpur A, Nundy M, Wang X, et al. The temporal association of introducing and lifting non-pharmaceutical interventions with the time-varying reproduction number (R) of SARS-CoV-2: a modelling study across 131 countries. Lancet Infect Dis. 2021;21: 193–202. doi:10.1016/S1473-3099(20)30785-4
5. Funk S, Camacho A, Kucharski AJ, Lowe R, Eggo RM, Edmunds WJ. Assessing the performance of real-time epidemic forecasts: A case study of Ebola in the Western Area region of Sierra Leone, 2014-15. PLoS Comput Biol. 2019;15: e1006785. doi:10.1371/journal.pcbi.1006785
6. Sabino EC, Buss LF, Carvalho MPS, Prete CA, Crispim MAE, Fraiji NA, et al. Resurgence of COVID-19 in Manaus, Brazil, despite high seroprevalence. Lancet. 2021;397: 452–455. doi:10.1016/S0140-6736(21)00183-5
7. Monod M, Blenkinsop A, Xi X, Hebert D, Bershan S, Tietze S, et al. Age groups that sustain resurging COVID-19 epidemics in the United States. Science. 2021;371. doi:10.1126/science.abe8372
8. Wallinga J, van Boven M, Lipsitch M. Optimizing infectious disease interventions during an emerging epidemic. Proc Natl Acad Sci USA. 2010;107: 923–928. doi:10.1073/pnas.0908491107
9. Brauner JM, Mindermann S, Sharma M, Johnston D, Salvatier J, Gavenčiak T, et al. Inferring the effectiveness of government interventions against COVID-19. Science. 2021;371. doi:10.1126/science.abd9338
10. Parag KV, Donnelly CA. Adaptive estimation for epidemic renewal and phylogenetic skyline models. Syst Biol. 2020;69: 1163–1179. doi:10.1093/sysbio/syaa035
11. Dehning J, Zierenberg J, Spitzner FP, Wibral M, Neto JP, Wilczek M, et al. Inferring change points in the spread of COVID-19 reveals the effectiveness of interventions. Science. 2020;369. doi:10.1126/science.abb9789
12. Johnson P, Moriarty J, Peskir G. Detecting changes in real-time data: a user's guide to optimal detection. Philos Trans A, Math Phys Eng Sci. 2017;375. doi:10.1098/rsta.2016.0298
13. Abbott S, Hellewell J, Thompson RN, Sherratt K, Gibbs HP, Bosse NI, et al. Estimating the time-varying reproduction number of SARS-CoV-2 using national and subnational case counts. Wellcome Open Res. 2020;5: 112. doi:10.12688/wellcomeopenres.16006.2
14. Gostic KM, McGough L, Baskerville EB, Abbott S, Joshi K, Tedijanto C, et al. Practical considerations for measuring the effective reproductive number, Rt. PLoS Comput Biol. 2020;16: e1008409. doi:10.1371/journal.pcbi.1008409
15. Parag KV. Improved estimation of time-varying reproduction numbers at low case incidence and between epidemic waves. PLoS Comput Biol. 2021;17: e1009347. doi: 10.1371/journal.pcbi.1009347
16. Riley S, Ainslie KEC, Eales O, Walters CE, Wang H, Atchison C, et al. Resurgence of SARS-CoV-2: Detection by community viral surveillance. Science. 2021;372: 990–995. doi:10.1126/science.abf0874
17. du Plessis L, McCrone JT, Zarebski AE, Hill V, Ruis C, Gutierrez B, et al. Establishment and lineage dynamics of the SARS-CoV-2 epidemic in the UK. Science. 2021;371: 708–712. doi:10.1126/science.abf2946
18. Hay JA, Kennedy-Shaffer L, Kanjilal S, Lennon NJ, Gabriel SB, Lipsitch M, et al. Estimating epidemiologic dynamics from cross-sectional viral load distributions. Science. 2021; doi:10.1126/science.abh0635
19. Casella F. Can the COVID-19 Epidemic Be Controlled on the Basis of Daily Test Reports? IEEE Control Syst Lett. 2021;5: 1079–1084. doi:10.1109/LCSYS.2020.3009912
20. Holmdahl I, Buckee C. Wrong but Useful - What Covid-19 Epidemiologic Models Can and Cannot Tell Us. N Engl J Med. 2020;383: 303–305. doi:10.1056/NEJMp2016822

21. Fraser C, Riley S, Anderson RM, Ferguson NM. Factors that make an infectious disease outbreak controllable. Proc Natl Acad Sci USA. 2004;101: 6146–6151. doi:10.1073/pnas.0307506101
22. Drake JM. Limits to forecasting precision for outbreaks of directly transmitted diseases. PLoS Med. 2006;3: e3. doi:10.1371/journal.pmed.0030003
23. Kahn R, Peak CM, Fernández-Gracia J, Hill A, Jambai A, Ganda L, et al. Incubation periods impact the spatial predictability of cholera and Ebola outbreaks in Sierra Leone. Proc Natl Acad Sci USA. 2020;117: 5067–5073. doi:10.1073/pnas.1913052117
24. Parag KV. Sub-spreading events limit the reliable elimination of heterogeneous epidemics. J R Soc Interface. 2021;18: 20210444. doi:10.1098/rsif.2021.0444
25. Scarpino S, Petri G. On the predictability of infectious disease outbreaks. Nat Comms. 2019;10.
26. Mercer GN, Glass K, Becker NG. Effective reproduction numbers are commonly overestimated early in a disease outbreak. Stat Med. 2011;30: 984–994. doi:10.1002/sim.4174
27. Britton T, Scalia Tomba G. Estimation in emerging epidemics: biases and remedies. J R Soc Interface. 2019;16: 20180670. doi:10.1098/rsif.2018.0670
28. Parag KV, Cowling BJ, Donnelly CA. Deciphering early-warning signals of the elimination and resurgence potential of SARS-CoV-2 from limited data at multiple scales. medRxiv. 2020; doi:10.1101/2020.11.23.20236968
29. Sarrka S. Bayesian Filtering and Smoothing. Cambridge, UK: Cambridge University Press; 2013.
30. Overview of Syndromic Surveillance What is Syndromic Surveillance? [Internet]. [cited 19 Aug 2021]. Available: https://www.cdc.gov/mmwr/preview/mmwrhtml/su5301a3.htm
31. Syndromic surveillance: systems and analyses - GOV.UK [Internet]. [cited 19 Aug 2021]. Available: https://www.gov.uk/government/collections/syndromic-surveillance-systems-and-analyses
32. Daughton CG. Wastewater surveillance for population-wide Covid-19: The present and future. Sci Total Environ. 2020;736: 139631. doi:10.1016/j.scitotenv.2020.139631
33. Lipsitch M, Finelli L, Heffernan RT, Leung GM, Redd SC, 2009 H1n1 Surveillance Group. Improving the evidence base for decision making during a pandemic: the example of 2009 influenza A/H1N1. Biosecur Bioterror. 2011;9: 89–115. doi:10.1089/bsp.2011.0007
34. Wallinga J, Teunis P. Different epidemic curves for severe acute respiratory syndrome reveal similar impacts of control measures. Am J Epidemiol. 2004;160: 509–516. doi:10.1093/aje/kwh255
35. Pei S, Kandula S, Shaman J. Differential effects of intervention timing on COVID-19 spread in the United States. Sci Adv. 2020;6. doi:10.1126/sciadv.abd6370
36. Morris DH, Rossine FW, Plotkin JB, Levin SA. Optimal, near-optimal, and robust epidemic control. Commun Phys. 2021;4: 78. doi:10.1038/s42005-021-00570-y
37. Fraser C. Estimating individual and household reproduction numbers in an emerging epidemic. PLoS One. 2007;2: e758. doi:10.1371/journal.pone.0000758
38. Wallinga J, Lipsitch M. How generation intervals shape the relationship between growth rates and reproductive numbers. Proc R Soc B. 2007;274: 599–604.
39. Parag KV, Donnelly CA. Using information theory to optimise epidemic models for real-time prediction and estimation. PLoS Comput Biol. 2020;16: e1007990. doi:10.1371/journal.pcbi.1007990
40. Grunwald P. The Minimum Description Length Principle. The MIT Press; 2007.
41. Snyder D, Miller M. Random Point Processes in Time and Space. 2nd ed. Springer-Verlag; 1991.
42. Van Kerkhove MD, Bento AI, Mills HL, Ferguson NM, Donnelly CA. A review of epidemiological parameters from Ebola outbreaks to inform early public health decision-making. Sci Data. 2015;2: 150019. doi:10.1038/sdata.2015.19
43. Ferguson N, Laydon D, Nedjati-Gilani G, Others. Impact of non-pharmaceutical interventions (NPIs) to reduce COVID- 19 mortality and healthcare demand. Imperial

College London; 2020.
44. Cevik M, Marcus JL, Buckee C, Smith TC. SARS-CoV-2 transmission dynamics should inform policy. Clin Infect Dis. 2020; doi:10.1093/cid/ciaa1442
45. Bialek W, Setayeshgar S. Physical limits to biochemical signaling. Proc Natl Acad Sci USA. 2005;102: 10040–10045. doi:10.1073/pnas.0504321102
46. Parag KV, Vinnicombe G. Point process analysis of noise in early invertebrate vision. PLoS Comput Biol. 2017;13: e1005687. doi:10.1371/journal.pcbi.1005687
47. Lestas I, Vinnicombe G, Paulsson J. Fundamental Limits on the Supression of Molecular Fluctuations. Nature. 2010;467: 174–8.
48. Polonsky J, Baidjoe A, Kamvar Z, Others. Outbreak analytics: a developing data science for informing the response to emerging pathogens. Phil Trans R Soc B. 2019;374: 20180276.
49. summary E. Reproduction number (R) and growth rate (r) of the COVID-19 epidemic in the UK: methods of.
50. Goldstein E, Dushoff J, Ma J, Plotkin JB, Earn DJD, Lipsitch M. Reconstructing influenza incidence by deconvolution of daily mortality time series. Proc Natl Acad Sci USA. 2009;106: 21825–21829. doi:10.1073/pnas.0902958106
51. Baker MG, Wilson N, Blakely T. Elimination could be the optimal response strategy for covid-19 and other emerging pandemic diseases. BMJ. 2020;371: m4907. doi:10.1136/bmj.m4907
52. Pellis L, Scarabel F, Stage HB, Overton CE, Chappell LHK, Fearon E, et al. Challenges in control of COVID-19: short doubling time and long delay to effect of interventions. Philos Trans R Soc Lond B, Biol Sci. 2021;376: 20200264. doi:10.1098/rstb.2020.0264
53. Parag KV, Thompson RN, Donnelly CA. Are epidemic growth rates more informative than reproduction numbers? medRxiv. 2021; doi:10.1101/2021.04.15.21255565
54. Watts DJ, Muhamad R, Medina DC, Dodds PS. Multiscale, resurgent epidemics in a hierarchical metapopulation model. Proc Natl Acad Sci USA. 2005;102: 11157–11162. doi:10.1073/pnas.0501226102
55. Koyama S, Horie T, Shinomoto S. Estimating the time-varying reproduction number of COVID-19 with a state-space method. PLoS Comput Biol. 2021;17: e1008679. doi:10.1371/journal.pcbi.1008679
56. Liu Q-H, Ajelli M, Aleta A, Merler S, Moreno Y, Vespignani A. Measurability of the epidemic reproduction number in data-driven contact networks. Proc Natl Acad Sci USA. 2018;115: 12680–12685. doi:10.1073/pnas.1811115115

Funding

KVP and CAD acknowledge funding from the MRC Centre for Global Infectious Disease Analysis (reference MR/R015600/1), jointly funded by the UK Medical Research Council (MRC) and the UK Foreign, Commonwealth & Development Office (FCDO), under the MRC/FCDO Concordat agreement and is also part of the EDCTP2 programme supported by the European Union. CAD thanks the UK National Institute for Health Research Health Protection Research Unit (NIHR HPRU) in Emerging and Zoonotic Infections in partnership with Public Health England (PHE) for funding (grant HPRU200907). The funders had no role in study design, data collection and analysis, decision to publish, or manuscript preparation.